Journal of Zhejiang University SCIENCE A
ISSN 1673-565X (Print); ISSN 1862-1775 (Online)
www.zju.edu.cn/jzus; www.springerlink.com
E-mail: jzus@zju.edu.cn

Catalytic properties of $CuO/Sn_{0.9}Ti_{0.1}O_2$ and $CuO/Sn_{0.7}Ti_{0.3}O_2$ in NO+CO reaction*

JIANG Xiao-yuan†, DU Feng, ZHANG Xu, JIA Yan-rong, ZHENG Xiao-ming

(*Institute of Catalysis, Faculty of Science, Zhejiang University, Hangzhou 310027, China*)

†E-mail: xyjiang@mail.hz.zj.cn

Received Jan. 20, 2007; revision accepted June 23, 2007

Abstract: Using $Sn_xTi_{1-x}O_2$ as carriers, $CuO/Sn_{0.9}Ti_{0.1}O_2$ and $CuO/Sn_{0.7}Ti_{0.3}O_2$ catalysts with different loading amounts of copper oxide (CuO) were prepared by an impregnation method. The catalytic properties of $CuO/Sn_{0.9}Ti_{0.1}O_2$ and $CuO/Sn_{0.7}Ti_{0.3}O_2$ were examined using a microreactor-gas chromatography (GC) NO+CO reaction system and the methods of BET (Brunauer-Emmett-Teller), TG-DTA (themogravimetric and differential thermal analysis), X-ray diffraction (XRD) and H_2-temperature programmed reduction (TPR). The results showed that NO conversions of $Sn_{0.9}Ti_{0.1}O_2$ and $Sn_{0.7}Ti_{0.3}O_2$ were 47.2% and 43.6% respectively, which increased to 95.3% and 90.9% at 6 wt% CuO loading. However, further increase in CuO loading caused a decrease in the catalytic activity. The nitrogen adsorption-desorption isotherm and pore-size distribution curve of $Sn_{0.9}Ti_{0.1}O_2$ and $Sn_{0.7}Ti_{0.3}O_2$ represented type IV of the BDDT (Brunauer, Deming, Deming and Teller) system and a typical mesoporous sample. There were two CuO diffraction peaks (2θ 35.5° and 38.7°), and the diffraction peak areas increased with increasing CuO loading. TPR analysis also detected three peaks (α, β and γ) from the CuO-loaded catalysts, suggesting that the α peak was the reduction of the highly dispersed copper oxide, the β peak was the reduction of the isolated copper oxide, and the γ peak was the reduction of crystal phase copper oxide. In addition, a fourth peak (δ) of the catalysts meant that the $Sn_xTi_{1-x}O_2$ mixed oxides could be reductive.

Key words: $Sn_xTi_{1-x}O_2$ mixed oxides, $CuO/Sn_xTi_{1-x}O_2$ catalysts, H_2 atmosphere pretreatment, NO+CO reaction
doi: 10.1631/jzus.2007.A1839 **Document code:** A **CLC number:** R733.7

INTRODUCTION

Nitrogen oxides (NO_x) are the major air pollutants in modern cities, and are largely due to the exhaust of automobiles. The elimination of NO_x by metal-oxide catalysts has been studied for many years. Tin oxide (SnO_2) is an n-type semiconductor widely used in sensors (Giakoumelou *et al*., 2006), and in oxidation catalysis and more recently in automotive exhaust (Auroux *et al*., 2000; Bennici and Gervasini, 2006; Gómez-García *et al*., 2005; Kung and Kung, 2000). SnO_2 was a good transition metal oxide for NO reduction in the presence of oxygen, as reported by Teraoka *et al*.(1993). According to (Sheintuch *et al*., 1989), the activities were improved dramatically when Pt or Pd was loaded on SnO_2. Liang *et al*.(2003) studied the reductive properties of SnO_2-Al_2O_3 and found that 71% NO is transformed at 350 °C. Liu *et al*.(2002) revealed that TiO_2-SnO_2 solid solutions had very high activity in SO_2+NO+CO reaction and that NO is converted completely at 350 °C. Although tin(IV) oxide exhibits redox catalytic properties, these may be modified substantially by the incorporation of heteroelements, e.g. copper, palladium and chromium. It is well known that tin oxide-based materials have activity in the CO/O_2 and CO/NO reactions. Boccuzzi *et al*.(1994) found high activity of Cu/TiO_2 catalyst at low temperature in NO+CO reaction. Hu *et al*.(2001) examined the activities of CuO supported on CeO_2 and γ-Al_2O_3, and ceria-modified γ-Al_2O_3 catalysts in NO+CO reaction at 200 °C, showing that the catalytic activities were in the order of CuO/CeO_2>CuO/CeO_2/Al_2O_3>CuO/γ-Al_2O_3. The findings might indicate that

* Project (No. Y504131) supported by the Natural Science Foundation of Zhejiang Province, China

the catalytic activities largely depended upon the surface dispersed copper oxide species and the strong interactions between CuO and the supports. Lou *et al*.(2003) studied the copper-based catalysts (e.g. CuO/CeO_2-TiO_2, $CuO/Ce_xTi_{1-x}O_2$) and suggested the species of Cu(+1) and Cu(0) were the activity sites for NO+CO reaction. Jiang *et al*.(2004a; 2004b) found the activity of NO decomposition was higher by CuO-ZrO_2/TiO_2 than by CuO/TiO_2 and that the addition of ZrO_2 caused changes in CuO species. $Sn_xTi_{1-x}O_2$ mixed oxides are known as photocatalyst, but little information is available on the catalytic properties of CuO/SnO_2-TiO_2 in NO+CO reaction.

In this work, $CuO/Sn_{0.9}Ti_{0.1}O_2$ and $CuO/Sn_{0.7}Ti_{0.3}O_2$ catalysts with different CuO loading were prepared by impregnating the carrier with aqueous solutions containing required amount of $Cu(NO_3)_2$. The activities of $CuO/Sn_{0.9}Ti_{0.1}O_2$ and $CuO/Sn_{0.7}Ti_{0.3}O_2$ catalysts were determined under the steady state in a fixed-bed quartz reactor, and the catalytic reducibility and characteristics were investigated using the methods of BET (Brunauer-Emmett-Teller), TG-DTA (themogravimetric and differential thermal analysis), XRD (X-ray diffraction) and H_2-TPR (temperature programmed reduction).

MATERIALS AND METHODS

Preparation of $Sn_{0.9}Ti_{0.1}O_2$ and $Sn_{0.7}Ti_{0.3}O_2$

$Sn_{0.9}Ti_{0.1}O_2$ and $Sn_{0.7}Ti_{0.3}O_2$ were prepared by coprecipitation method from $SnO_2{\cdot}5H_2O$ and $TiCl_4$ with ammonia solution as precipitating reagent. Appropriate quantity of $SnO_2{\cdot}5H_2O$ and $TiCl_4$ solutions were mixed at a proper Sn/Ti ratio, and then added to aqueous ammonia until pH=9 was reached and an intensive precipitation occurred. After precipitation, the products were aged for 36 h and then filtrated by vacuum pump and washed with 0.5 mol/L of NH_4NO_3 solution until no Cl^- was detected with 0.1 mol/L AgCl. The resulting precipitations was dried at 110 °C for 24 h and then calcined at 450 °C in air stream for 2 h.

Catalyst preparation

$CuO/Sn_{0.9}Ti_{0.1}O_2$ and $CuO/Sn_{0.7}Ti_{0.3}O_2$ catalysts were prepared by impregnation method using $Cu(NO_3)_2$ aqueous solution of desired concentrations. The impregnation lasted for 24 h. The obtained catalysts were dried, and then calcined at 500 °C in air stream for 2 h.

Catalytic activity measurement and analysis

Catalytic activity was determined under the steady state in a fixed-bed quartz reactor (6 mm). The particle size of catalysts was 20~40 mesh, and 120 mg of the catalysts were used. The reaction gas (i.e. feed steam) consisted of a fixed composition of 6.0% NO, 6.0% CO and 88% He (v/v) as a dilute. The catalysts were pretreated in NO+CO reaction stream at 50 °C for 0.5 h. After being cooled to room temperature, they were allowed to react with the mixed gas. The reactions occurred at different temperatures at space velocity of 5000 h^{-1}. Two column and thermal conduction detectors were used for analyzing the catalytic activity. Column *A* was packed with 13X molecular sieve for separating N_2, NO and CO, and Column *B* was packed with Paropak Q for separating N_2O and CO_2.

Characterization

The specific surface areas, pore size distribution and adoption-desorption isotherms were determined by the nitrogen adsorption isotherms at 77 K using a Coulter OMNISORP-100 instrument.

The TG-DTA experiment was carried out using PE Corp TG-DTA comprehensive thermal analyser. About 10 mg of each sample was taken and measured in air atmosphere. The TG-DTA spectra were obtained with temperature ramped at a linear heating rate of 20 °C/min.

XRD data were obtained at 25 °C using a horizontal Rigaku B/Max lllB powder diffractometer with CuK_α radiation and a power of 40×30 mA.

H_2-TPR was done by gas chromatography (GC) using a thermal conductivity detector. The sample (5~10 mg) was activated in an O_2 stream at 500 °C for 0.5 h. After being cooled to 30 °C, H_2-TPR was conducted.

RESULTS

Textural and structural properties of carrier and catalysts

The specific surface areas of catalysts increased with the increase in CuO loading (Table 1). In addition, the specific surface areas of $Sn_{0.9}Ti_{0.1}O_2$ and

Table 1 Specific surface area of the carriers and catalysts

Carriers and catalysts (I)	Specific surface area (m^2/g)	Carriers and catalysts (II)	Specific surface area (m^2/g)
$Sn_{0.9}Ti_{0.1}O_2$	47.3	$Sn_{0.7}Ti_{0.3}O_2$	109.2
6 wt% $CuO/Sn_{0.9}Ti_{0.1}O_2$	42.7	6 wt% $CuO/Sn_{0.7}Ti_{0.3}O_2$	79.3
12 wt% $CuO/Sn_{0.9}Ti_{0.1}O_2$	40.9	12 wt% $CuO/Sn_{0.7}Ti_{0.3}O_2$	69.4
24 wt% $CuO/Sn_{0.9}Ti_{0.1}O_2$	37.4	24 wt% $CuO/Sn_{0.7}Ti_{0.3}O_2$	38.8

$CuO/Sn_{0.9}Ti_{0.1}O_2$ with different CuO loadings were smaller than those of $Sn_{0.7}Ti_{0.3}O_2$ and $CuO/Sn_{0.7}Ti_{0.3}O_2$ respectively. This was likely due to pure crystallite SnO_2, which had specific surface area of only 26.6 m^2/g. The influence of Sn is always crucial for the increase of rutile/anatase ratio that largely determines the size of crystallites (Oliveira *et al*., 2003). Therefore, the incorporation of Sn in this study could justify the small size of the rutile. In contrast, anatase crystallites are larger than for undoped, especially for calcined samples, indicating a low incorporation of Sn into the particles of the anatase. $Sn_{0.9}Ti_{0.1}O_2$ has a small specific surface area, and as CuO loading increased the specific surface area changed slowly. By comparison, $Sn_{0.7}Ti_{0.3}O_2$ has less amount of pure crystal SnO_2 and thus much larger specific surface area, and as CuO loading increased the specific surface area showed a big decrease.

As shown in Figs.1 and 2, the samples of $Sn_{0.9}Ti_{0.1}O_2$ and $Sn_{0.7}Ti_{0.3}O_2$ were porous and their N_2 isotherms belonged to type IV, a typical mesoporous material. $Sn_{0.9}Ti_{0.1}O_2$ has a single pore size, but $Sn_{0.7}Ti_{0.3}O_2$ has two pore sizes. We suggest that SnO_2 is well-dispersed on $Sn_{0.9}Ti_{0.1}O_2$, compared with only isolated SnO_2 dispersion on $Sn_{0.7}Ti_{0.3}O_2$.

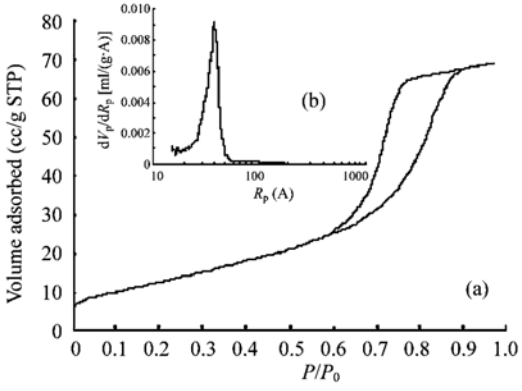

Fig.1 Adsorption-desorption isotherms (a) and pore size distribution (b) of $Sn_{0.9}Ti_{0.1}O_2$

STP: standard temperature and pressure; R_p: pore radius; V_p: pore volume; P: pressure of adsorption balance; P_0: saturation vapor pressure

TG-DTA measurement

The thermal behavior of $Sn_{0.9}Ti_{0.1}O_2$ during heating process occurred below 800 °C (Fig.3a). There was an endothermic peak at 190 °C, with the corresponding TGA (themogravimetric analysis) curve showing less weight. Since the evaporative temperature of H_2O is 100 °C, the endothermic peak was the results of evaporation and removal of the adsorbed water. The peak followed the loss of weakly bonded water located in the interlayer space at >250 °C. At the same time, the energy changed as $Sn_{0.9}Ti_{0.1}O_2$ atoms renewed combination. Sensato *et al*.(2003) and Fresno *et al*.(2005) found that the bonding energy increased from 2.9 to 3.3 eV when x changed from 0 to 1 in $Sn_xTi_{1-x}O_2$ solid solution. In this study, an exothermic peak was observed at about 500 °C, indicating the completion of anatase crystallization. Above 500 °C, there was no exothermic peak and the anatase transformation was a gradual progress.

During the TGA of $Sn_{0.7}Ti_{0.3}O_2$, one weight loss was detected between 80 and 200 °C (Fig.3b). The corresponding DTA (differential thermal analysis) profile in fresh samples showed an endothermic peak of dehydration at 200 °C. By comparing Figs.3a and 3b, there was a distinct weight reduction after 100 °C. Besides dehydration, NH_4NO_3 may also decompose at high temperature. The appearance of exothermic peaks at about 500 °C also indicated a completion of anatase crystallization.

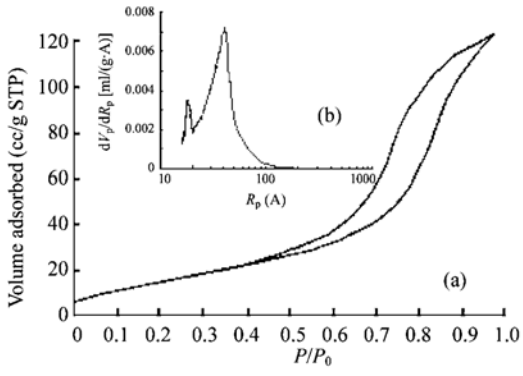

Fig.2 Adsorption-desorption isotherms (a) and pore size distribution (b) of $Sn_{0.7}Ti_{0.3}O_2$

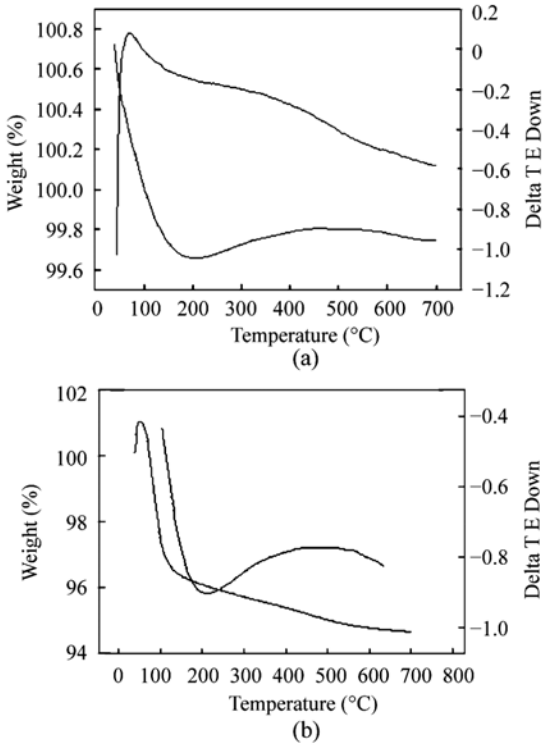

Fig.3 TG-DTA profile of $Sn_{0.9}Ti_{0.1}O_2$ (a) and $Sn_{0.7}Ti_{0.3}O_2$ (b)

XRD analysis

After calcination at 450 °C, the peak of $Sn_{0.9}Ti_{0.1}O_2$ was higher and narrower than that of $Sn_{0.7}Ti_{0.3}O_2$ (Fig.4). Kong *et al*.(2002) found the XRD peak of crystallite SnO_2 or TiO_2 was higher and narrower than $Sn_{0.5}Ti_{0.5}O_2$ compound oxide. The tin proportion in $Sn_{0.9}Ti_{0.1}O_2$ was higher than that in $Sn_{0.7}Ti_{0.3}O_2$, which probably shaped a certain amount of SnO_2 crystallite in $Sn_{0.9}Ti_{0.1}O_2$.

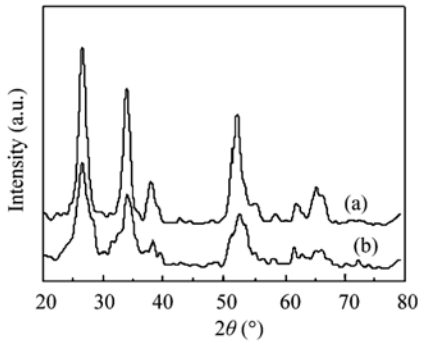

Fig.4 XRD patterns of $Sn_{0.9}Ti_{0.1}O_2$ (a) and $Sn_{0.7}Ti_{0.3}O_2$ (b)

As shown in Fig.5a, two CuO diffraction peaks of $CuO/Sn_{0.9}Ti_{0.1}O_2$ were detected (2θ 35.5° and 38.7°). At 6 wt% CuO loading, the peaks were very narrow. With increment of CuO loading, the diffraction peaks of CuO were higher and narrower, indicating that crystallite CuO increased and that excessive CuO formed the bulk CuO particles. Previous studies reported that the incorporation of Sn facilitated the formation of rutile crystallites (Kumar *et al*., 1993; Kulshreshtha *et al*., 2001). In our study, however, no rutile crystallite was detected but only anatase, probably due to the low calcination temperature and preparation method.

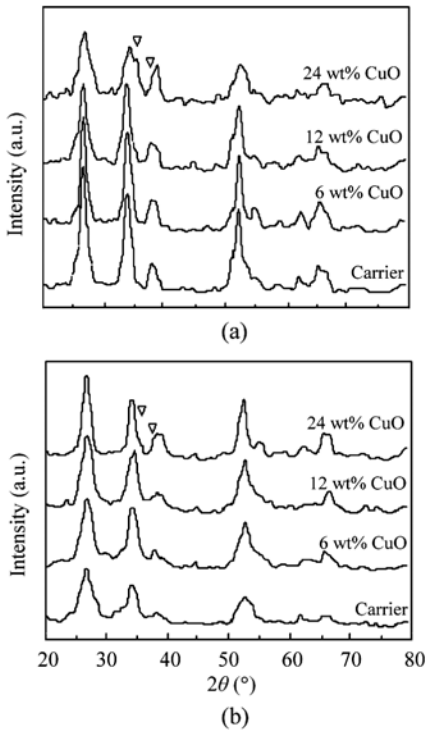

Fig.5 XRD patterns of $CuO/Sn_{0.9}Ti_{0.1}O_2$ (a) and $CuO/Sn_{0.7}Ti_{0.3}O_2$ (b) with different CuO loadings. ∇: CuO

Two CuO diffraction peaks (2θ 35.5° and 38.7°) of $CuO/Sn_{0.7}Ti_{0.3}O_2$ also became higher and narrower with increase in CuO loading (Fig.5b). Only anatase was detected. CuO loading had less effect on $Sn_{0.7}Ti_{0.3}O_2$ than on $Sn_{0.9}Ti_{0.1}O_2$, probably because the former had larger specific surface area than the latter.

NO+CO reaction

The catalytic activities in NO+CO reaction by $CuO/Sn_{0.9}Ti_{0.1}O_2$ and $CuO/Sn_{0.7}Ti_{0.3}O_2$ are shown in Figs.6a and 6b. The activity of $Sn_{0.9}Ti_{0.1}O_2$ and $Sn_{0.7}Ti_{0.3}O_2$ was quite low and NO conversion was 47.2% and 43.6% respectively. By comparison, NO conversion increased to 95.3% and 90.9% at 6 wt%

CuO loading, and the activity was plateaued or even decreased at reaction temperature of 200~300 °C. Further increase in CuO loading caused a decrease in the catalytic activity. According to (Kulshreshtha *et al*., 2001), SnO_2 became completely inactive at <360 °C, and NO conversion was only observed above 360 °C. In NO+CO reaction, a certain amount of SnO_2 had no effect but mixed oxide played a role in low temperature, and both affected the reaction at high temperature. When CuO was loaded on $Sn_{0.9}Ti_{0.1}O_2$ or $Sn_{0.7}Ti_{0.3}O_2$, the activity improved sharply.

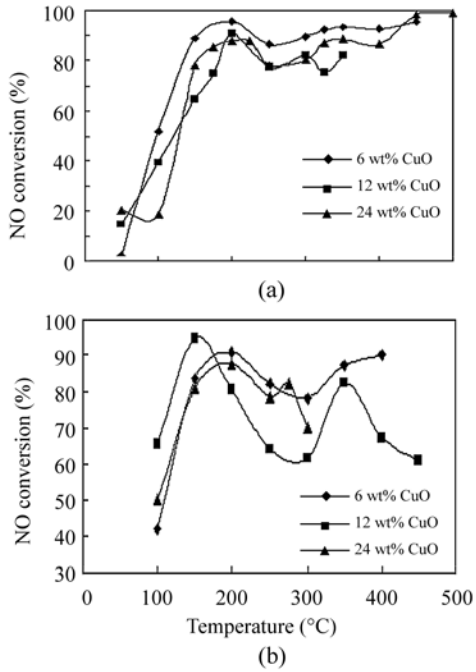

Fig.6 Activities of $CuO/Sn_{0.9}Ti_{0.1}O_2$ (a) and $CuO/Sn_{0.7}Ti_{0.3}O_2$ (b) with different CuO loadings in air atmosphere

It was found that NO conversion increased with increasing temperature until 200 °C, but little N_2O, N_2 or CO_2 was detected. Fu *et al.*(1991) concluded that Cu^{2+} was the active site of NO adsorption but Cu^{+} was the active site of CO adsorption, and suggested that after NO and CO were absorbed, the desorption process firstly produced N_2O and then N_2. In terms of Langmuir-Hinshelwood mechanisms, both NO and CO are adsorbed prior to the reaction. Therefore, NO conversion is supposed to be complete transformation with NO adsorption being the major process until 200 °C.

CO is consumed at the completion of reaction by $CuO/Sn_{0.7}Ti_{0.3}O_2$. During the reaction, NO conversion decreased sharply. In (Solymosi and Kiss, 1976), pure SnO_2 prefers the oxidation of CO to the reduction, and it is regarded that is the lattice oxygen which leads to this phenomenon. They classified the lattice oxygen into three species: the surface lattice oxygen, the second layer lattice oxygen and the deeper layer lattice oxygen. Surface lattice oxygen contacted with CO directly. In reductive process, it should be reduced firstly, followed by the second layer. The lattice oxygen may lead to CO transformation prior to NO at the near completion of reaction. When $CuO/Sn_{0.7}Ti_{0.3}O_2$ was pretreated in H_2 atmosphere at 500 °C, NO selectivity and high temperature activity improved (Fig.7). NO conversion reached 100% on the catalysts of 12 wt% and 24 wt% $CuO/Sn_{0.7}Ti_{0.3}O_2$ at 450 °C. Whereas, NO conversion reached 90% on the catalysts of 6 wt% $CuO/Sn_{0.7}Ti_{0.3}O_2$ at 500 °C.

The activity of 24 wt% $CuO/Sn_{0.7}Ti_{0.3}O_2$ was examined at different pretreatment temperatures (Fig.8). After pretreatments at 150 °C and 250 °C, NO conversion was 80.1% and 100% respectively. When 24 wt% $CuO/Sn_{0.7}Ti_{0.3}O_2$ was pretreated at 100 °C, NO conversion was 80.1%, similar to the activity of catalyst pretreated at 250 °C, but had very low NO selectivity and 98.5% NO conversion. The other H_2

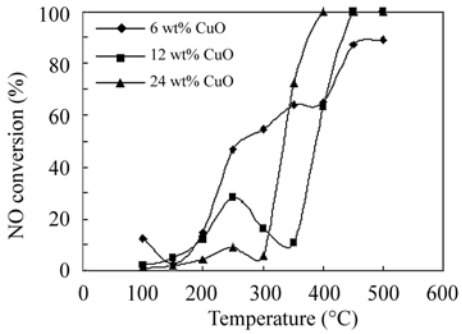

Fig.7 Activities of $CuO/Sn_{0.7}Ti_{0.3}O_2$ with different CuO loadings after reduction pretreatment at different temperatures

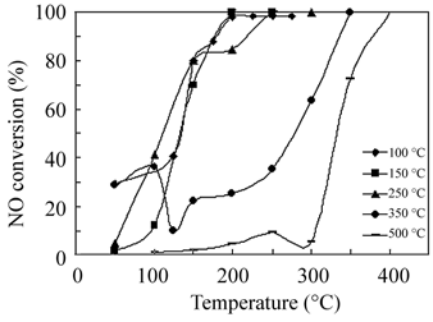

Fig.8 Activities of 24 wt% $CuO/Sn_{0.7}Ti_{0.3}O_2$ after reduction pretreatment at different temperatures

pretreated temperatures did not improve the catalytic activity.

H_2-TPR of catalysts

The H_2-TPR profile of $CuO/Sn_{0.9}Ti_{0.1}O_2$ showed four reduction peaks, while $Sn_{0.9}Ti_{0.1}O_2$ had only one reduction peak (Fig.9a). The single peak of $Sn_{0.9}Ti_{0.1}O_2$ (δ) occurred at 660 °C. When CuO was loaded, the δ peak size became augmented and the reduction temperature decreased, indicating an existence of pure SnO_2 crystallite. $Sn_{0.9}Ti_{0.1}O_2$ with well-dispersed SnO_2 was more reductive after CuO loading. Another three peaks were detected (α peak at 185 °C, β peak at 207 °C and γ peak at 440 °C) at 6 wt% CuO loading. When CuO loading increased to 12 wt% and 24 wt%, α peak occurred at higher temperatures (188 and 200 °C, respectively) and β peak temperature also changed, but γ peak temperature showed little variation. Xu *et al.*(1998) found Cu^{2+} ions with significantly different reducibility on the anatase surface. Larsson *et al.*(1996) suggested that at low temperature, 3 wt% CuO/TiO_2 contained Cu^+, 12 wt% CuO/TiO_2 contained Cu^{2+}, and CuO crystalline existed at high CuO/TiO_2. According to (Coq *et al*., 1995), isolated Cu^{2+} ions were more active than CuO

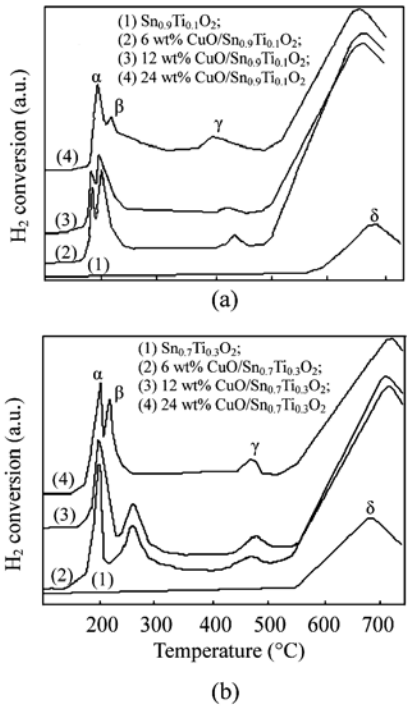

Fig.9 H_2-TPR profile of $CuO/Sn_{0.9}Ti_{0.1}O_2$ (a) and $CuO/Sn_{0.7}Ti_{0.3}O_2$ (b) with different CuO loadings

clusters or protons for the selective reduction of NO. The reduction of Cu^{2+} species occurs in two steps: $Cu^{2+}\rightarrow Cu^+$ at around 510 K and $Cu^+\rightarrow Cu^0$ between 600 and 700 K. Córdoba *et al*.(1998) reported four types of CuO on CuO/TiO_2: the bulk CuO, the chain stabilization forms of Cu^{2+} ions and two different oxide clusters with a structure similar to CuO. We suggest that α, β and γ peaks all show CuO reduction behavior on $Sn_{0.9}Ti_{0.1}O_2$. The α peak was part of the reduction of highly dispersed CuO, the β peak was part of the reduction of the isolated copper oxide interacting with $Sn_{0.9}Ti_{0.1}O_2$, and the γ peak was the reduction of the crystallite copper oxide. Except for the adsorption at low temperature, the reaction activity corresponded to CuO increment, indicating that CuO crystallite plays an important role in reaction activity. Fig.9b shows the reduction behavior of $Sn_{0.7}Ti_{0.3}O_2$ and $CuO/Sn_{0.7}Ti_{0.3}O_2$ with three CuO loading. $Sn_{0.7}Ti_{0.3}O_2$ was reduced at 660~670 °C (δ peak). After CuO was loaded, the δ peak area increased and α, β and γ peaks occurred at relatively low temperatures. The reduction temperature of α peak increased with increasing CuO loading (187, 188 and 191 °C at 6 wt%, 12 wt% and 24 wt% CuO loading, respectively). At 6 wt% and 12 wt% CuO loading β peak occurred at 250 °C, while at 24 wt% CuO loading the peak temperature was 211 °C. In contrast, the reduction temperature of γ peak was 460~470 °C and was not affected by the amount of CuO loading.

CONCLUSION

(1) The catalytic activity of 6 wt% $CuO/Sn_{0.9}Ti_{0.1}O_2$ was higher than that of $CuO/Sn_{0.7}Ti_{0.3}O_2$. NO conversions by $Sn_{0.9}Ti_{0.1}O_2$ and $Sn_{0.7}Ti_{0.3}O_2$ alone were 47.2 and 43.6% respectively, but increased to 95.3% and 90.9% at 6 wt% CuO loading. Further increase in CuO loading caused a decrease in the catalytic activity.

(2) CuO diffraction peaks occurred at 2θ 35.5° and 38.7°, and only anatase was detected. The crystallite CuO had greater diffraction peak and higher activity in NO+CO reaction as CuO loading increased.

(3) Three peaks (α, β and γ) were detected when CuO was loaded on $Sn_{0.9}Ti_{0.1}O_2$ and $Sn_{0.7}Ti_{0.3}O_2$. The α, β and γ peaks were due to the reduction of highly

dispersed CuO, the isolated CuO interacting with $Sn_xTi_{1-x}O_2$ and the crystalline copper oxide, respectively. The δ peak was the reduction of the carrier.

References

Auroux, A., Sprinceana, D., Gervasini, A., 2000. Support effects on de-NO_x catalytic properties of supported tin oxides. *J. Catal.*, **195**(1):140-150. [doi:10.1006/jcat.2000.2970]

Bennici, S., Gervasini, A., 2006. Catalytic activity of dispersed CuO phases towards nitrogen oxides (N_2O, NO, and NO_2). *Applied Catalysis B: Environmental*, **62**(3-4):336-344. [doi:10.1016/j.apcatb.2005.09.001]

Boccuzzi, F., Guglielminotti, E., Martra, G., Cerrato, G., 1994. Nitric oxide reduction by CO on Cu/TiO_2 catalysts. *J. Catal.*, **146**(2):449-459. [doi:10.1006/jcat.1994.1082]

Coq, B., Tachon, D., Figuéras, F., Mabilon, G., Prigent, M., 1995. Selective catalytic reduction of nitrogen monoxide by decane on copper exchanged mordenites. *Applied Catalysis B: Environmental*, **6**(3):271-289. [doi:10.1016/0926-3373(95)00018-6]

Córdoba, G., Viniegra, M., Fierro, J.G., Palilla, J., Arroyo, R., 1998. TPR, ESR and XPS study of Cu^{2+} ions in sol-derived TiO_2. *J. Solid. State Chem.*, **138**(1):1-6. [doi:10.1006/jssc.1997.7690]

Fresno, F., Coronado, J.M., Tudela., D., Soria, J., 2005. Influence of the structural characteristics of $Ti_{1-x}Sn_xO_2$ nanoparticles on their photocatalytic the elimination of methylcyclohexanc vapors. *Applied Catalysis B: Environmental*, **55**(3):159-167. [doi:10.1016/j.apcatb.2004.07.012]

Fu, Y.L., Yang, C., Lin, P.Y., 1991. A low-temperature IR spectroscopic study of selective adsorption of NO and CO on CuO/γ-Al_2O_3. *J. Catal.*, **132**(1):85-91. [doi:10.1016/0021-9517(91)90249-4]

Giakoumelou, I., Fountzoula, C., Kordulis, C., Boghosian, S., 2006. Molecular structure and catalytic activity of V_2O_5/TiO_2 catalysts for the SCR of NO by NH_3: In situ Raman spectra in the presence of O_2, NH_3, NO, H_2O, and SO_2. *J. Catal.*, **239**(1):1-12. [doi:10.1016/j.jcat.2006.01.019]

Gómez-García, M.A., Pitchon, V., Kiennemann, A., 2005. Removal of NO_x from lean exhaust gas by storage/reduction on $H_3PW_{12}O_{40}{\cdot}6H_2O$ supported on $Ce_xZr_{4-x}O_8$. *Exviron. Sci. Technol.*, **39**(2):638-644. [doi:10.1021/es0498641]

Hu, Y.H., Dong, L., Shen, M.M., Liu, D., Wang, J., Ding, W.P., Chen, Y., 2001. Influence of supports on he activities of copper oxide species in the low-temperature NO+CO reaction. *Applied Catalysis B: Environmental*, **31**(1):61-69. [doi:10.1016/S0926-3373(00)00269-1]

Jiang, X.Y., Lou, L.P., Chen, Y.X., Zheng, X.M., 2004a. Preparation and characterization of $Ce_{0.3}Ti_{0.7}O_2$ and supported CuO catalysts for NO+CO reaction. *Catal. Lett.*, **94**(1-2):49-55. [doi:10.1023/B:CATL.0000019330.20466.87]

Jiang, X.Y., Ding, G.H., Lou, L.P., Chen, Y.X., Zheng, X.M., 2004b. Catalytic activities of CuO/TiO_2 and $CuO\text{-}ZrO_2/TiO_2$ in NO+CO reaction. *J. Mol. Catal. A: Chemical*, **218**(2):187-195. [doi:10.1016/j.molcata.2004.02.020]

Kong, L.B., Ma, J., Huang, H., 2002. Low temperature formation of yttrium aluminum garnet from oxides via a high-energy ball milling process. *Mater. Lett.*, **56**(3):344-348. [doi:10.1016/S0167-577X(02)00480-9]

Kulshreshtha, S.K., Sasikala, R., Sudarsan, V., 2001. Non-random distribution of cations in $Sn_{1-x}Ti_xO_2$ ($0.0 \le x \le 1.0$): A ^{119}Sn MAS NMR study. *J. Mater. Chem.*, **11**(3):930-935. [doi:10.1039/b006258h]

Kumar, K.P., Keizer, K., Burggraaf, A.J., 1993. Textural evolution and phase-transformation in titania membranes. *J. Mater. Chem.*, **3**(11):1141-1149. [doi:10.1039/jm9930301141]

Kung, M.C., Kung, H.H., 2000. Lean NO_x catalysis over alumina-supported catalysts. *Top. Catal.*, **10**(1-2):21-26. [doi:10.1023/A:1019147630269]

Larsson, P.O., Anddersson, A., Wallenberg, L.R., Svensson, B., 1996. Combustion of CO and toluene: characterization of copper oxide supported on titania and activity comparisons with supported cobalt iron and manganese oxide. *J. Catal.*, **163**(2):279-293. [doi:10.1006/jcat.1996.0329]

Liang, J.F., Ma, J., Liu, Z.Q., Yang, X.Y., 2003. TPR and TPD Research of deSO_x and deNO_x integration catalyst SnO_2-TiO_2. *J. Mol. Catal.*, **17**(5):353-356 (in Chinese).

Liu, Z.Q., Ma, J., Zhang, Z.L., Yang, X.Y., 2002. The reaction mechanism of SO_2, NO and CO on the $Sn_{0.5}Ti_{0.5}O_2$ catalysts. *Acta Physico-Chimica Sinica*, **18**(3):193-196 (in Chinese).

Lou, L.P., Jiang, X.Y., Chen, Y.X., Lu, G.L., Zhou, R.X., Zheng, X.M., 2003. $Ce_xTi_{1-x}O_2$ mixed oxides supported CuO catalyst for NO reduction by CO. *Journal of Rare Earths*, **21**(3):331-336 (in Chinese).

Oliveira, M.M., Schnitzler, D.C., Zarbin, A.J., 2003. $(Ti,Sn)O_2$ mixed oxides nanoparticles obtained by the sol-gel route. *Chem. Mater.*, **15**(9):1903-1909. [doi:10.1021/cm021034 4]

Sensato, F.R., Custodio, R., Longo, E., Beltrán, A., Andrés, J., 2003. Electronic and structural properties of $Sn_xTi_{1-x}O_2$ solid solutions: A periodic DFT study. *Catal. Today*, **85**(2-4):145-152. [doi:10.1016/S0920-5861(03)00382-1]

Sheintuch, M., Schmidt, J., Lecthman, Y., Yahav, G., 1989. Modelling catalyst-support interactions in carbon monoxide catalysed by Pb/SnO_2. *Appl. Catal.*, **49**(1):55-65. [doi:10.1016/S0166-9834(00)81421-9]

Solymosi, F., Kiss, J., 1976. Adsorption and reduction of NO on tin(IV) oxide catalysts. *J. Catal.*, **41**(2):202-211. [doi:10.1016/0021-9517(76)90335-3]

Teraoka, Y., Harada, T., Iwasaki, T., 1993. Selective reduction of nitrogen monoxide with hydrocarbons over SnO_2 catalyst. *Chem. Lett.*, **22**(5):773-776. [doi:10.1246/cl.1993.773]

Xu, B., Dong, L., Chen, Y., 1998. Influence of CuO loading on dispersion and reduction behavior of CuO/TiO_2 (anatase) system. *Chem. Soc. Faraday Trans.*, **94**(13):1905-1909. [doi:10.1039/a801603h]